

“NaB₁₅”: A New Structural Description Based on X-ray and Neutron Diffraction, Electron Microscopy, and Solid-State NMR Spectroscopy

Barbara Albert,^{*[a]} Kathrin Hofmann,^[a] Christian Fild,^[b] Hellmut Eckert,^[b] Michaela Schleifer,^[c] and Reginald Gruehn^[c]

Abstract: A boron-rich sodium boride, formerly known as NaB₁₅, has been subjected to a comprehensive structural reinvestigation using X-ray single-crystal and powder diffraction, low-temperature neutron and electron diffraction, high-resolution transmission electron microscopy, and ²³Na solid-state NMR spectroscopy. The results indicate that the previously published orthorhombic space group is incorrect. Consistent with all of the experimental results a modified structural description is developed in the monoclinic space group *I*m*m*1 (*a* = 585.92(3), *b* = 1039.92(6), *c* = 833.17(5) pm, β = 90.373(5)° from powder data). Because one of the interstitial boron atom positions remains unoccupied, the accurate compositional formula is NaB_{14.5} or Na₂B₂₉.

Keywords: boron • electron microscopy • neutron diffraction • NMR spectroscopy • structure elucidation

Introduction

Very few compounds exist that are well-defined products of reactions in the binary sodium/boron system. So far, the crystal structures of only two binary sodium borides have been published. These are Na₃B₂₀, whose structure was solved only recently by X-ray^[1] and neutron^[2] powder diffraction methods, and NaB₁₅, reported in the form of small single crystals by Naslain et al. about thirty years ago.^[3–5] Its structure consists of slightly distorted B₁₂ icosahedra, which are interconnected directly and through additional boron interstitials, thereby forming a very rigid framework of boron atoms. Similar to other icosahedral boron-rich solids, for example boron suboxide B₆O which was reinvestigated recently by Hubert et al.,^[6] NaB₁₅ is a material that exhibits considerable hardness.

The structural model which was suggested^[4] earlier by Naslain and Kasper is shown in Figure 1. The authors chose an

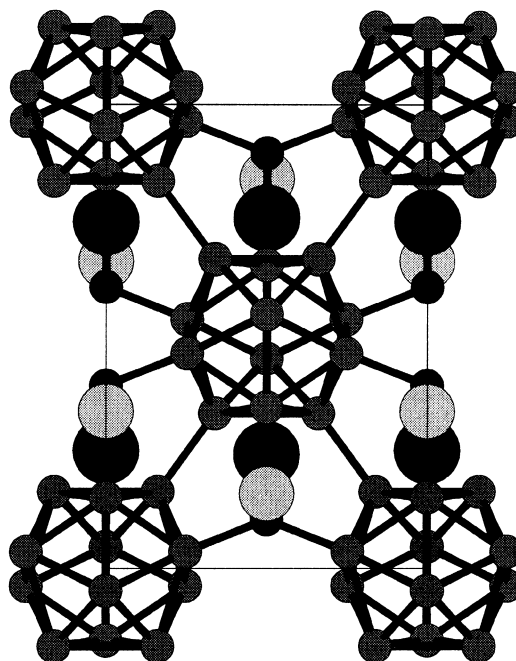


Figure 1. Crystal structure plot^[9] of “NaB₁₅” in *Im*11 (*a* = 584.7, *b* = 841.5, *c* = 1029.8 pm) according to Naslain and Kasper^[4], view along [001] (gray: icosahedral boron atoms; black: interstitial boron atoms; light gray: sodium atoms).

orthorhombic space group (*Im*m, No. 74) with *a* = 584.7, *b* = 841.5, and *c* = 1029.8 pm (306 independent reflections, *R* value 0.08). The “most probable”^[4] formula for the boron-rich compound under investigation—first^[3] described as NaB₁₆ or

[a] Dr. B. Albert, Dipl.-Chem. K. Hofmann
Institut für Anorganische und Analytische Chemie I
Justus-Liebig-Universität
Heinrich-Buff-Ring 58, 35392 Giessen (Germany)
Fax: (+49) 641-9934109
E-mail: barbara.albert@anorg.chemie.uni-giessen.de

[b] Dipl.-Chem. C. Fild, Prof. Dr. H. Eckert
Institut für Physikalische Chemie, Westfälische Wilhelms-Universität
Schlossplatz 7, 48149 Münster (Germany)

[c] Dipl.-Chem. M. Schleifer, Prof. Dr. R. Gruehn
Institut für Anorganische und Analytische Chemie II
Justus-Liebig-Universität
Heinrich-Buff-Ring 58, 35392 Giessen (Germany)

ϕ phase—was derived by crystallographical considerations to be NaB_{15} , of which four units were found in the unit cell. It is important to emphasize that according to this description the asymmetric unit contains only a single sodium atom position.

The analysis of boron-rich compounds is rather complicated and may result in incorrect and/or misleading compositional and structural descriptions of the compounds. Well-known examples are the impurity-stabilized “allotropes” of boron, B_{50}N_2 or B_{50}C_2 .^[7,8] Therefore, in the study of such materials, the usage of complementary techniques is a mandatory requirement. Concerning the previously reported structure of NaB_{15} it is evident from Figure 1 that the localization of some of the interstitial boron atoms is not satisfactory, which manifests itself in high thermal displacement parameters. The large uncertainty in this boron position suggests a picture more averaged than necessary. In the present study, we address this issue within a comprehensive structural investigation using X-ray single-crystal and powder diffraction, low-temperature neutron and electron diffraction, high-resolution transmission electron microscopy (HRTEM), and ^{23}Na solid-state NMR spectroscopy. Based on these complementary techniques we propose a new structural model consistent with all of the data.

Results and Discussion

Our attempts at refining the earlier published^[4] structural model for NaB_{15} on the basis of our X-ray and neutron powder diagrams were unsuccessful for both the centrosymmetric space groups $Imma$ and $Immm$ and the noncentrosymmetric space groups $Ima2$ and $Imm2$, producing very large thermal displacement parameters for some of the interstitial boron atoms even at 2 K (neutron data). Furthermore, the high R values obtained suggested an incorrect space group. Repeating the refine-

ment on a newly acquired single crystal (Figure 2) data set led to no better results. The possibility that NaB_{15} is in fact a compound stabilized by impurities was excluded by probing for elements other than sodium or boron using electron

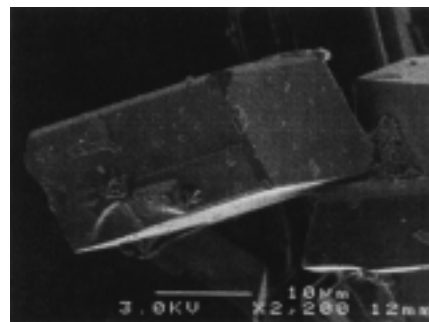


Figure 2. Scanning electron micrograph of Na_2B_{29} .

energy loss spectroscopy (EELS), energy-dispersive X-ray analysis (EDX), magnetic measurements, and ^1H NMR spectroscopy. These findings indicate that the problem is crystallographic in origin, suggesting that the actual symmetry of NaB_{15} is lower than previously believed. This question is addressed directly by ^{23}Na solid-state NMR spectroscopy.

The ^{23}Na triple-quantum (TQ) magic angle spinning (MAS) NMR spectrum is shown in Figure 3. Clearly, two distinct sites are visible at isotropic chemical shifts of $\delta = 10.2$ and 16.9 (versus 1M NaCl solution) and nuclear electric quadrupolar

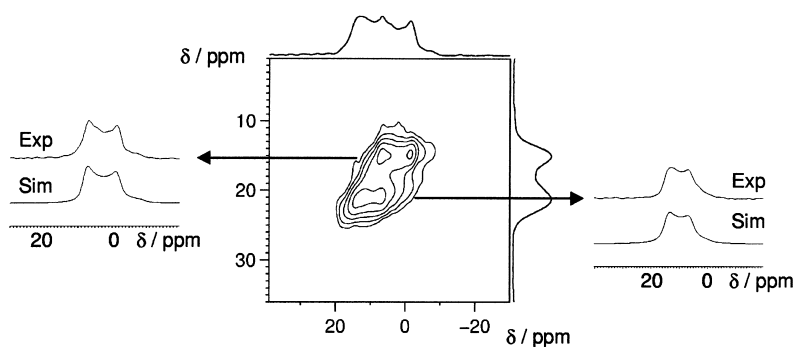


Figure 3. 132.3 MHz ^{23}Na triple-quantum MAS NMR spectrum with two components extracted and simulated.

Abstract in German: Ein borreiches Natriumborid, bisher bekannt als NaB_{15} , wurde mittels Röntgenbeugung an Pulver und Einkristall, Tieftemperaturneutronen- und Elektronenbeugung, hochauflösender Transmissionselektronenmikroskopie und ^{23}Na Festkörper-NMR-Spektroskopie strukturell umfassend charakterisiert. Die Ergebnisse zeigen, daß die früher publizierte Raumgruppe nicht richtig ist. Eine modifizierte Strukturbeschreibung, die in Übereinstimmung mit allen experimentellen Ergebnissen steht, wurde in der Raumgruppe $Im1$ ($a = 585.92(3)$, $b = 1039.92(6)$, $c = 833.17(5)$ pm, $\beta = 90.373(5)^\circ$ aus Pulverdaten) entwickelt. Weil eine der interstitiellen Boratompositionen nicht mehr besetzt ist, muß die genaue Zusammensetzung der Verbindung durch die Summenformel $\text{NaB}_{14.5}$ bzw. Na_2B_{29} angegeben werden.

coupling constants of 2.4 and 2.2 MHz, respectively. Based on these spectroscopic parameters the MAS NMR spectrum can be fitted by two powder patterns with equal areas (Figure 4), revealing unambiguously that there are two almost equally occupied independent sodium positions in the crystal structure. $^{23}\text{Na}\{^{11}\text{B}\}$ rotational echo double resonance (REDOR) experiments are summarized in Figure 5. Figure 5a plots the normalized ^{23}Na MAS spin echo attenuation $(S_o - S)/S_o$, effected by the 180° pulses applied to the ^{11}B resonance, as a function of the dipolar evolution time. The steep increase of $(S_o - S)/S_o$ is consistent with the presence of strong ^{11}B - ^{23}Na heteronuclear dipole-dipole couplings. Figure 5b compares Fourier transforms of the free induction decays corresponding to S and S_o at two different evolution times. The simulations of all of these four line shapes indicate that the population ratios for the two sodium sites are identical within experimental

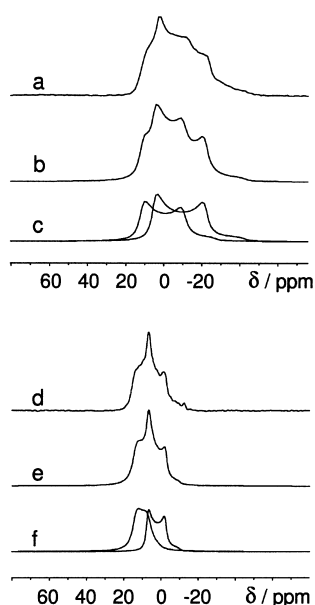


Figure 4. ^{23}Na MAS spectrum at 79.4 MHz (a: observed, b: simulated, c: individual components in the simulation) and 132.3 MHz (d: observed, e: simulated, f: individual components in the simulation). The small spike observed near $\delta = -12$ in the latter spectrum is an experimental artefact.

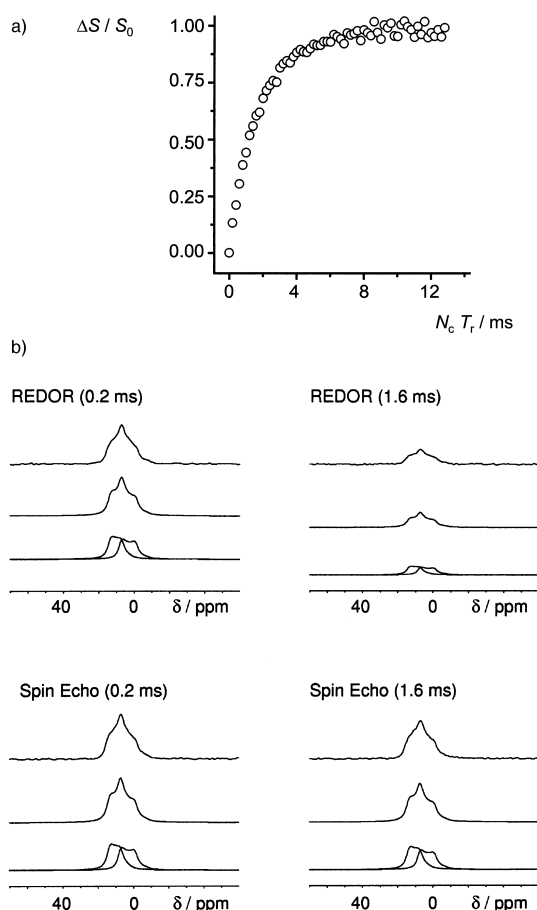


Figure 5. a) Plot of the ^{23}Na spin echo attenuation $(S_0 - S)/S_0$ against the dipolar evolution time $N_c T_R$ (no. of rotor cycles times length of the rotor period) for the $^{23}\text{Na}\{^{11}\text{B}\}$ REDOR spectra shown in b. b) Comparison of ^{23}Na spin echo and $^{23}\text{Na}\{^{11}\text{B}\}$ REDOR Fourier transforms for two different dipolar evolution times (top trace: observed; middle: simulated; bottom: individual components in the simulation).

error. These results confirm that both types of sodium atoms experience very similar dipolar coupling strengths with the ^{11}B nuclei.

The clear presence of two independent sodium positions in the crystal structure reflects a reduction in the symmetry in the structural description of NaB_{15} . Two hypotheses can be discussed: either, the conditions of body (I) centering are violated, or, the crystal system turns out to be monoclinic instead of orthorhombic with the angle β close to 90° . The first scenario is ruled out on the basis of electron diffraction (Figure 6) and neutron diffraction results, both of which give no indication of deviations from I type centering. By electron diffraction, the dimensions of the unit cell ($a = 580$, $b = 1020$, $c = 830$ pm, $\beta \approx 90^\circ$) are confirmed. We therefore conclude that the symmetry of NaB_{15} is monoclinic. The deviation from orthorhombic symmetry then is directly connected with the positions and/or occupancies of the interstitial boron sites.

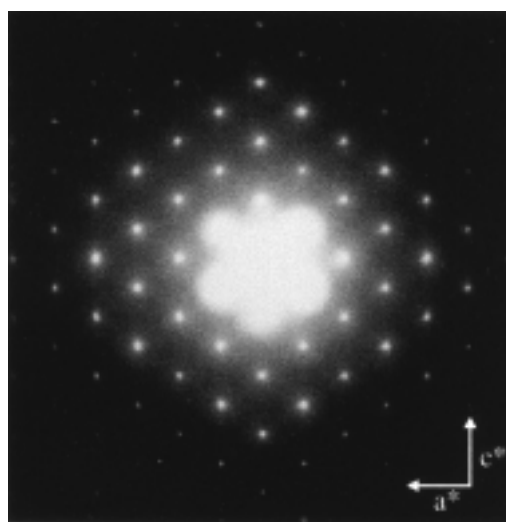


Figure 6. Electron diffraction pattern of Na_2B_{29} along $[010]$.

Using the single-crystal data set, we re-solved the structure by direct methods and refined it in the space group $I1m1$ (Cm , No. 7). Since β is close to 90° , pseudo-merohedral twinning of the monoclinic components can emulate orthorhombic symmetry. Therefore, the twin law was introduced during the refinement (matrix $100,0\bar{1}0,00\bar{1}$) and the fractional contribution of the two components was refined to 0.55 and 0.45. Owing to the high pseudo-symmetry of the structure, the thermal displacement parameters of the boron atoms were refined isotropically. The resulting atomic arrangement is shown in Figure 7. Further details concerning the structure analysis are given in Table 1.

It is evident that the arrangement of the sodium and of the icosahedral boron atoms, as well as of some of the interstitial boron atoms is very similar to that found by Naslain and Kasper.^[4] The main result of our structure analysis is the following: the position of the interstitial boron atom which exhibits a large thermal displacement parameter in space group $I1m1$ now splits into two positions, of which only one is occupied by boron atoms. The other one remains empty. So, instead of four sodium and sixty boron atoms present per unit

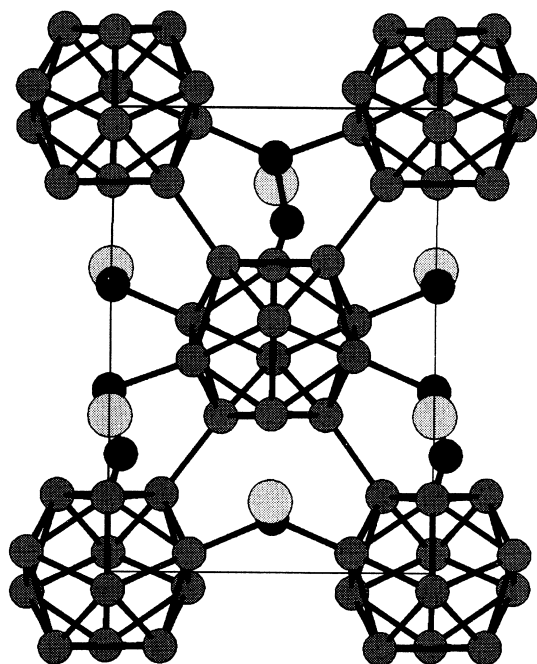


Figure 7. Crystal structure plot^[9] of Na_2B_{29} in $I1m1$ ($a = 587.4$, $b = 1040.3$, $c = 835.9$ pm, $\beta = 90.17^\circ$), view along $[010]$ (gray: icosahedral boron atoms; black: interstitial boron atoms, light gray: sodium atoms).

Table 1. Details of the single-crystal structure analysis for Na_2B_{29} .

formula	Na_2B_{29}
M [g mol^{-1}]	359.50
crystal system	monoclinic
space group	$I1m1$ (no. 7)
a [pm]	587.4(1)
b [pm]	1040.3(1)
c [pm]	835.9(2)
β [$^\circ$]	90.17(3)
V [10^6 pm^3]	511(1)
Z	4
ρ_{calcd} [g cm^{-3}]	2.336
$F(000)$	333.9
μ [mm^{-1}]	0.17
h, k, l	$\pm 7, \pm 12, \pm 10$
no. of observed reflections	4588
no. of unique reflections	1089
R_{int}	0.0559
refined parameters	75
R indices	
$wR(F^2)$	0.2197
$R(F)$	0.1016 (all reflections)
$R(F)$	0.0729 (801 reflections with $F > 4\sigma(F)$)
min./max. residual electron density [$\text{e } \text{\AA}^{-3}$]	$-0.58/1.20$

cell, there are four sodium and only fifty-eight boron atoms. The compositional formula for the investigated compound now has to be written as $\text{NaB}_{14.5}$ or Na_2B_{29} instead of NaB_{15} . Consistent with the ^{23}Na MAS NMR spectrum, the structure contains two inequivalent sodium sites with equal populations. The chemical shift difference between the corresponding resonances reflects the change in the local sodium atom environment caused by the reduced boron occupancy in the interstitial site. Interestingly, our new compositional assignment agrees quite well with the results of the chemical

analysis ($\text{Na}:\text{B} = 1:14.6$) performed by the authors of the earlier structural model.^[4]

Since there were indications for a systematic pseudo-merohedral twinning of the single crystals, we repeated Rietveld refinements of the X-ray and neutron data now using the monoclinic structural model. The fits between observed and calculated data are satisfactory, as can be seen in Figures 8 and 9. The positional parameters are shifted only slightly compared with the single-crystal data refinement. Further refinement information is given in Table 2.

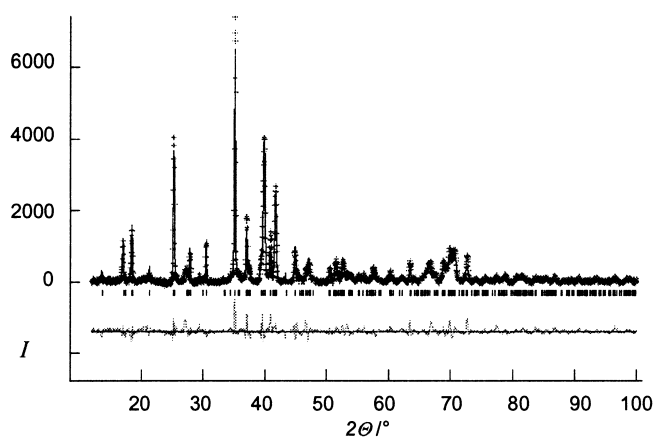


Figure 8. Observed (+) and calculated (solid line) X-ray powder diffraction pattern of Na_2B_{29} with the difference curve (bottom). The vertical dashes indicate the positions of reflections. I = Intensity.

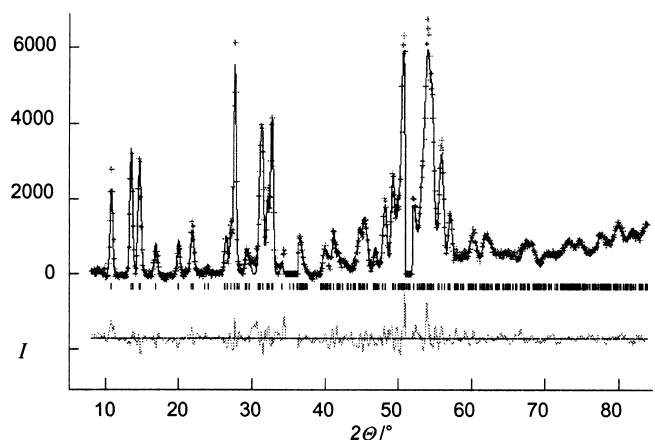


Figure 9. Observed (+) and calculated (solid line) neutron powder diffraction pattern of Na_2B_{29} with the difference curve (bottom). The vertical dashes indicate the positions of reflections. I = Intensity.

The HRTEM images (Figure 10) show a projection of the structure along $[010]$ for different values of the defocus. The dark spots on the image which was taken near the Scherzer defocus at -650 \AA can be very nicely assigned to the boron atom icosahedra. The simulations of the images (Table 3), which are shown as inserts, have been calculated on basis of the corrected monoclinic structural model. The agreement between the observed and calculated images is very convincing.

Table 2. Crystal data and structure powder refinement parameters for Na₂B₂₉.

	X-ray diffraction	Neutron diffraction
empirical formula		Na ₂ B ₂₉
temperature [°C]	20.0(5)	–271.5(3)
wavelength [Å]	1.54056	1.218
unit cell dimensions		
<i>a</i> [pm]	585.92(3) ^[a]	585.7(1)
<i>b</i> [pm]	1039.92(6)	1039.8(2)
<i>c</i> [pm]	833.17(5)	833.7(2)
β [°]	90.373(5)	90.8(2)
<i>Z</i>		4
used 2θ range	12–100	8–84
No. observed reflections	326	405
<i>R</i> _{wp}	0.1056	0.0709
<i>R</i> _p	0.0785	0.0533
ρ_{\min}/ρ_{\max} [e Å ^{–3}]	–0.60/0.77	–

[a] Low standard deviations for lattice parameters result from the data treatment in the structure refinement program; the real values are probably less precise, but nevertheless comparable in accuracy.

Conclusion

The boron-rich sodium boride previously described as “NaB₁₅” actually contains sodium and boron in a 2:29 ratio. It crystallizes in the monoclinic system. The symmetry reduction from space group *Imam* to *I1m1* is necessary to account for the presence of two independent sodium positions. The present study illustrates the power of the combined application of different structural techniques with complementary informational contents.

Experimental Section

Synthesis: Sodium (Merck, Darmstadt, p. a.) was refined by segregation and sealed in glass ampoules. Boron was either used as purchased (amorphous modification, Chempur, Karlsruhe, 99.9+ %) or pretreated for 16 h at 1000 °C and 3×10^{-3} mbar (¹¹B isotope 99%, β -crystalline modification, Chemtrade, Düsseldorf). Typically, about 0.3 g of sodium and 0.2 g of boron were filled into a pre-boronated tantalum tube, which was sealed under helium by arc welding and exposed to reaction conditions (1050 °C, 3 h, plus 1150 °C, 3 h). After reaction, an excess of sodium was removed by distillation at 10^{-2} mbar and 350 °C. All of the starting materials and the product were handled in an argon atmosphere, although the product did not prove to be air-sensitive.

Characterization: Samples were checked for identification and crystallinity by X-ray powder diffraction (Huber Guinier diffractometer G645, Cu_{K α} radiation, quartz monochromator). Magnetic measurements conducted on a Faraday balance between room temperature and –269.75 °C revealed diamagnetic behavior. ¹H MAS NMR obtained on a Bruker DSX-500 spectrometer indicated the absence of hydrogen-containing impurities. The ¹¹B MAS NMR spectrum showed a broad, poorly resolved signal centered near $\delta = 8$ versus BF₃(OEt)₂ which was not further analyzed. Scanning electron microscopy (SEM) using a JEOL JSM-6300F electron microscope at 2.0 kV indicated crystal edge lengths of approximately 50 μ m.

Single-crystal data: A small crystal ($0.076 \times 0.038 \times 0.057$ mm³) was sealed in a glass capillary and investigated using an image plate diffraction system (Stoe, Mo_{K α} , graphite monochromator, 295 K, 4588 reflections collected in the range of $4^\circ < 2\theta < 56^\circ$). Structure solution applying direct methods and full-matrix least-squares refinement against *F*² was performed using the SHELXS^[10] and SHELXL^[11] program systems. Further details of the crystal structure investigation may be obtained from the Fachinformationszentrum Karlsruhe, 76344 Eggenstein-Leopoldshafen (Germany) on quoting the depository number CSD-410920.

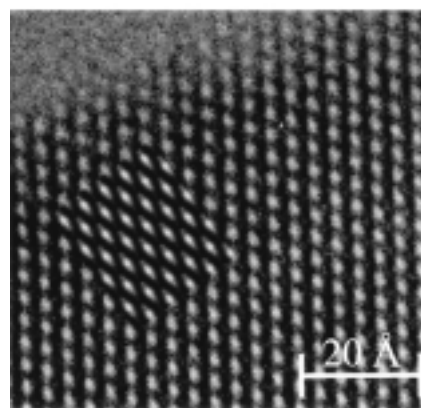
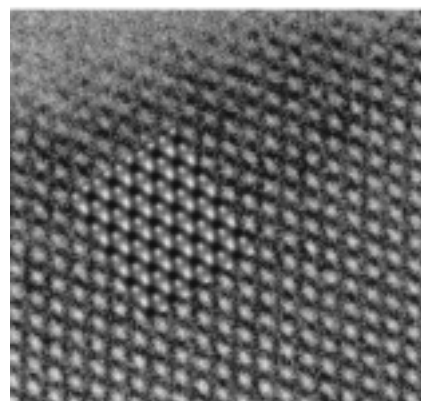
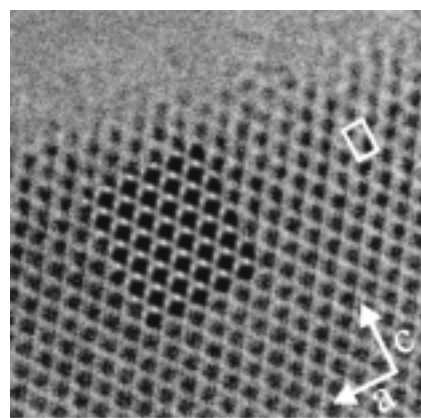


Figure 10. HRTEM images of Na₂B₂₉ for different values of the defocus ($\epsilon = -650, -800, -1020$ Å). Projection along [010]; the contrast simulations are shown in the inserts, the unit cell is indicated by white lines. The crystal thickness along [010] is 6.23 nm.

Table 3. Parameters for contrast simulations of HRTEM images of Na₂B₂₉.

Objective lens aperture	10 nm ^{–1}
spherical aberration coefficient	1.2 nm
spread of focus	80 nm
chromatic aberration	0.8 mrad
crystal thickness along [010]	6.23 nm

X-ray and neutron powder diffraction: X-ray powder data were collected using a flat-plate sample holder sitting in a thermally equilibrated and evacuated chamber (5×10^{-5} mbar) and running from $\theta = 3$ to 50° with a step size of 0.01° . The low-temperature neutron data were collected for an isotopically pure $\text{Na}^{11}\text{B}_{15}$ sample between $2\theta = 5$ to 84° with a step size of 0.1° at the E2 beam line, Hahn-Meitner-Institut, Berlin. The sample was filled in air-tight vanadium containers. The refinement of the two data sets was performed by using the GSAS program package.^[12] The cut-off for peaks is 0.1% of the peak maximum for the X-ray data, and 1% for the neutron data. The background of the X-ray pattern was corrected using a 36 parameter cosine Fourier function. The profile function used is a modified pseudo-Voigt function with six parameters refined. The neutron data were refined correcting the background with a 12 parameter cosine Fourier function. A standard Gaussian function modified for peak asymmetry was used for the profile refining six parameters. Two reflections that stemmed from the aluminum dewar vessel had to be cut out of the neutron data set. For both data sets the zero point and a scale factor were refined.

HRTEM investigations: The sample was crushed in an agate mortar down to a particle diameter of about 10 μm . The HRTEM specimens were placed on a lacey carbon-coated copper TEM grid and set in a transmission electron microscope operated at 300 kV (Philips CM30ST) equipped with a double-tilt holder. Contrast simulations were performed with the program EMS^[13] using the experimental parameters summarized in Table 3. A Gatan PEELS666 spectrometer was used for the electron energy loss spectroscopy (EELS) experiment and a PVSUPQ system (Philips) for the energy dispersive X-ray spectroscopy experiment (EDX). The EDX spectrum proved the absence of elements with $Z > 11$. The EEL spectra of several particles confirmed the absence of light-element impurities.

^{23}Na solid-state NMR spectroscopy: ^{23}Na MAS NMR spectra were obtained at 132.3 MHz, and 79.4 MHz, using Bruker DSX-500 and CXP-300 spectrometers, respectively. Samples were rotated at a spinning frequency of 12 kHz, using standard 4 mm Bruker MAS probes. MQ MAS NMR spectra were obtained with the three-pulse ZQ-filtering sequence,^[14] using experimental conditions reported previously.^[15] Triple-quantum coherence was excited by a hard pulse of 4.60 μs length. The evolution time was incremented in steps of 3 μs and stopped by a second hard pulse of 1.25 μs length. Signal detection followed subsequent to a third pulse of 8.0 μs length. A 5 s recycle delay was used.

For $^{23}\text{Na}^{[11]\text{B}}$ rotational echo double resonance (REDOR) spectroscopy the pulse sequence of Gullion and Schaefer^[16] was used. Resonance frequencies were 132.3 and 160.5 MHz for ^{23}Na and ^{11}B , respectively. Experiments were conducted at a spinning frequency of 10 kHz using a Bruker triple resonance probe. 90° pulse lengths were 5 and 2.8 μs for ^{23}Na and ^{11}B , respectively and a relaxation delay of 7 s was used. Detailed

inspection of the REDOR data revealed no differences in dephasing behavior between the two sodium sites, indicating comparable $^{11}\text{B} - ^{23}\text{Na}$ heteronuclear dipolar interaction strengths.

Acknowledgements

B.A. and K.H. are very grateful to Prof. Dr. J. Beck, Bonn, for his interest and help. Support for this work was provided by the Land Hessen (research stipend for K.H.), the Land Nordrhein-Westfalen (NMR spectrometer), as well as by the Fonds der Chemischen Industrie (research stipend for C.F.), and the Deutsche Forschungsgemeinschaft (transmission electron microscope and AL 536/1-1). Single data collection was performed by G. Koch. Dr. Thomas Zeiske, Berlin, assisted the neutron data collection, which was supported by the Hahn-Meitner-Institut, Berlin.

- [1] B. Albert, *Angew. Chem.* **1998**, *110*, 1135; *Angew. Chem. Int. Ed.* **1998**, *37*, 1117.
- [2] B. Albert, K. Hofmann, *Z. Anorg. Allg. Chem.* **1998**, *625*, 709.
- [3] P. Hagenmuller, R. Naslain, *Compt. Rend.* **1963**, *257*, 1294.
- [4] R. Naslain, J. S. Kasper, *J. Solid State Chem.* **1970**, *1*, 150.
- [5] R. Naslain, A. Guette, P. Hagenmuller, *J. Less-Common Met.* **1976**, *47*, 1.
- [6] H. Hubert, B. Devouard, L. A. J. Garvie, M. O'Keeffe, P. R. Buseck, W. T. Petuskey, P. F. McMillan, *Nature* **1998**, *391*, 376.
- [7] K. Ploog, H. Schmidt, E. Amberger, G. Will, K. H. Kossobutzki, *J. Less-Common Met.* **1972**, *29*, 161.
- [8] G. Will, K. Ploog, *Nature* **1974**, *251*, 406.
- [9] R. Hundt, Program KPLOT, Bonn, Germany, **1979**.
- [10] G. M. Sheldrick, Program SHELXS-86, Göttingen, Germany, **1986**.
- [11] G. M. Sheldrick, Program SHELXL-98, Göttingen, Germany, **1998**.
- [12] A. C. Larson, R. B. Von Dreele, Program GSAS, Los Alamos, USA, **1985**.
- [13] P. A. Stadelmann, *Ultramicroscopy* **1987**, *21*, 131.
- [14] J. P. Amoureux, C. Fernandez, S. Steuernagel, *J. Magn. Reson. A* **1996**, *123*, 116.
- [15] L. Züchner, J. C. C. Chan, W. Müller-Warmuth, H. Eckert, *J. Phys. Chem.* **1998**, *112*, 4495.
- [16] T. Gullion, J. Schaefer, *J. Magn. Reson.* **1989**, *81*, 196.

Received: August 23, 1999 [F1992]